Thermodynamically Stable β[Ni(Al,Ti)]-β'[Ni_2AlTi]-γ'[Ni_3(Al,Ti)] Metal-Metal Composites

L.C. HSIUNG and H.K.D.H. BHADESHIA

Single-phase intermetallic compounds are often quite brittle. Experiments are reported in which a metallic composite consisting of three different intermetallic compounds (β, β', and γ') in the Ni-Ti-Al system was fabricated by extruding a mechanical mixture of the compounds. In this way, the microstructure could be engineered to disperse the most ductile intermetallic in between the more brittle components. An additional feature was to choose the β, β', and γ' powders with compositions which allowed them to coexist in equilibrium when coextruded to form the composite. It is found that this approach confers elevated temperature microstructural stability, a crack arresting ability, reasonable ductility, and considerable strength even at high temperatures.

I. INTRODUCTION

RELATIVELY brittle phases can sometimes be exploited by dispersing them in a ductile matrix. A higher ductility can then be obtained from the overall microstructure. Some well-known examples include martensitic steels in which austenite retained between the plates of martensite can be beneficial to the overall mechanical properties.[1,2] Cermets, such as composites of WC-Co[3] and Al_2O_3-Al,[4] also rely on this principle.

Recent work[5] on the Ni-Al-Ti system indicates that alloys consisting of a three-phase mixture of β, β', and γ', have the capability of considerable strength at high temperatures, as well as a promising level of ductility at room temperature. These phases are all ordered intermetallic compounds; β–Ni(Al,Ti) has the B2 structure, β–Ni_2AlTi has the $L2_1$ structure, and γ'-Ni_3(Al,Ti) has the $L1_2$ structure. The β phase can be described as an ordered body-centered cubic structure in which the Al and Ti atoms are randomly dispersed at the body centering sites. The β' structure is a further modification of this, in which the Al and Ti order on their sublattice, and the compound is often called a Heusler compound. The γ' phase can be described as an ordered face-centered cubic structure. On their own, each of these compounds can be quite brittle, but the β and β' phases are particularly brittle.

Yang *et al.*,[6] in their study of three-phase β, β', and γ', reported significant ambient temperature ductility for microstructures produced by heat treatment of cast alloys. However, there is a limited amount of control that can be exercised when generating microstructures by solid state precipitation induced by heat treatment. Our aim in the present work was instead to engineer the microstructure by separately manufacturing the individual phases, then using extrusion as a method of consolidating them. The idea was to disperse films of the more ductile γ' between the brittle β and β' compounds in order to achieve greater ductility while at the same time retaining the strength advantage of a three-phase mixture. It is, of course, desirable for the resulting microstructure to be stable at elevated temperatures, where the material might eventually be used. Therefore, the compositions of the individual phases were chosen to correspond to the corners of a tie-triangle of the equilibrium phase diagram. In this way, irrespective of the proportions in which the individual phases are combined before extrusion, there should be no tendency for any of the elements to redistribute between the phases. Previous researchers[7] have coextruded different intermetallic compounds, but have not considered the thermodynamic stability of the resulting microstructure.

II. EXPERIMENTAL PROCEDURE

Figure 1 shows an isothermal section (900 °C) of the Ni-rich corner of Ni-Al-Ti phase diagram, as obtained experimentally by Yang *et al.*[6] The position of the triangle does change with temperature, but the change is not large, so the three powders (pure β, β', and γ') were made with their respective compositions given by the corners of the 900 °C tie-triangle. A tie-triangle represents the compositions of phases which are in equilibrium (Table I), so that any microstructure made using these three powders should be in thermodynamic equilibrium (at least at 900 °C). The phases can be consolidated by extrusion to form a metal–metal composite (MeMeC), whose microstructure is controlled by the fabrication process rather than by precipitation reactions.

Two such composites, designated MeMeC *B* and MeMeC *C*, were made using powders whose compositions are given in Table II. The experimental powders were prepared and analyzed at Ishikawajima–Harima Heavy Industries (IHI), Japan, using argon atomization, and were sieved (150 μm) in air. The atomization process for γ' was particularly difficult, with a large amount of flakes being produced. After mixing of different weight percentages of γ', β, and β' powders (MeMeC *B*: 50γ'-25β-25β', MeMeC *C*: 70γ'-15β-15β', all in wt pct), the mechanical mixtures were sent to the International Nickel Corporation (INCO), United Kingdom, for extrusion. Table III lists the extrusion conditions.

The γ', β, and β' powders were studied using an X-ray

L.C. HSIUNG, Postgraduate Research Student, and H.K.D.H. BHADESHIA, Reader in Physical Metallurgy, are with the Department of Materials Science and Metallurgy, University of Cambridge, Cambridge, United Kingdom.

Manuscript submitted October 13, 1994.

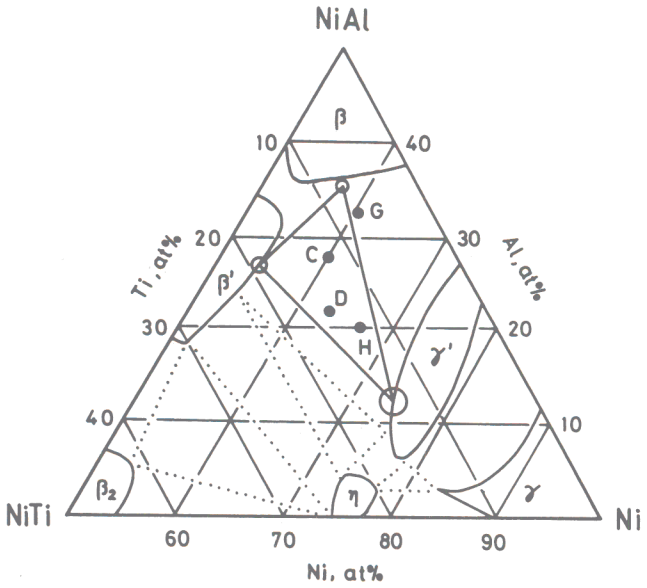

Fig. 1 — Isothermal section (900 °C) of the three-phase (β + β' + γ') region. The circles represent the margin of error in the compositions of the three phases, as determined from alloys *C* and *D*.[6]

Table I. Compositions (Atomic Percent) of the Three Corners of a γ'-β'-β Tie-Triangle[6]

Phase	Ni	Al	Ti
γ'	72.7	12.9	14.4
β'	53.2	25.1	21.7
β	56.5	35.9	7.6

Table II. Compositions (Atomic Percent) of the Three Alloy Powders

Powder	Ni	Al	Ti
γ'	73.61	11.91	14.48
β'	53.37	25.77	20.86
β	57.24	36.65	6.11

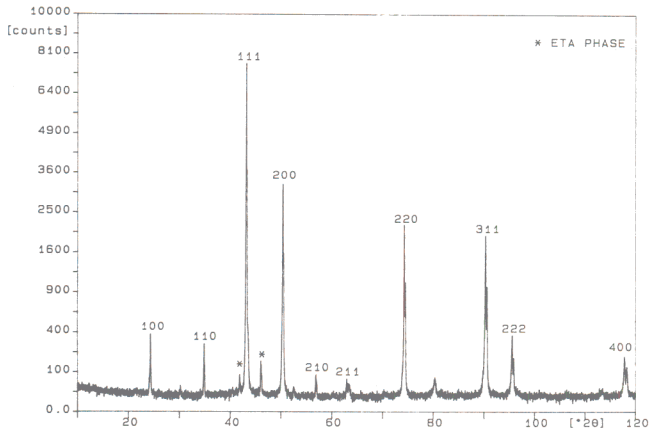

Fig. 2 — X-ray diffraction pattern of γ'-phase $Ni_3(Al, Ti)$ powders.

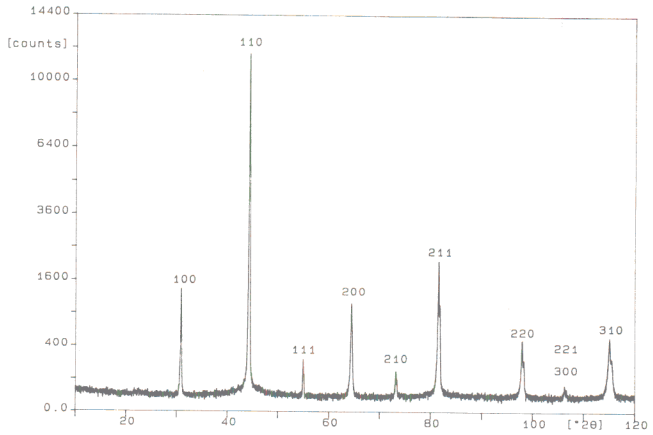

Fig. 3 — X-ray diffraction pattern of β-phase Ni(Al, Ti) powders.

diffractometer (XRD) with Cu K_α (doublet λ = 1.5406 and 1.54439 Å) radiation.

During extrusion, the powders were canned in steel. To remove the steel from the extruded bars, each sample was, after cutting, soaked in an aqueous solution of 30 pct HNO_3, 30 pct HCl for pickling. Samples for heat treatment were cut from the extruded bar and sealed in silica tubes, evacuated, and backfilled with some argon. All samples were cooled in air following heat treatment. Metallographic samples from both as-extruded and heat-treated materials were prepared, etched in Kalling's reagent, and examined under the optical microscopy. The composition of each phase in the as-extruded and heat-treated samples was measured using an energy dispersive X-ray analyzer (EDX) in a scanning electron microscope (SEM). Hardness measurements were carried out using a Vickers hardness testing machine with a load of 20 kg.

Samples for room and elevated temperature compression testing were cut from heat-treated materials along longitudinal and transverse directions using an electro-discharge machine (EDM) into rectangular shapes having the dimensions of about 3.2 × 3.2 × 6 mm. Before testing, the specimens were mechanically polished using 1200 grit SiC paper. Compression tests were performed using a MAYES* 50 KN servohydraulic machine, testing in air at room temperature and 700 °C at an engineering strain rate of 2.3×10^{-4} s^{-1}. Samples that failed after compression testing were examined using scanning electron microscopy to observe the fracture surfaces.

*MAYES is a trademark of Mayes Ltd., Windsor, United Kingdom.

III. RESULTS AND DISCUSSION

A. *Characterization of Alloy Powders*

X-ray diffraction results of the three kinds of powders with approximate compositions of the γ', β, and β' phases are shown in Figures 2 through 4. The pattern of the powder intended to be pure γ' (Figure 2) also shows the presence of small quantities of β, β', and the hexagonal closed-packed η phase Ni_3Ti. The additional phases are

Table III. Extrusion Conditions of MeMeC *B* and MeMeC *C

Alloy	Wt Pct	Preheat	Lubrication	Ram Speed
MeMeC *B*	$50\gamma'25\beta25\beta'$	1120 °C for 1 h	E-glass and fiber glass	35.5 mm s^{-1}
MeMeC *C*	$70\gamma'15\beta15\beta'$	1120 °C for 70 min	E-glass and fiber glass	25.1 mm s^{-1}

*The extrusion ratio in each case is 16:1.

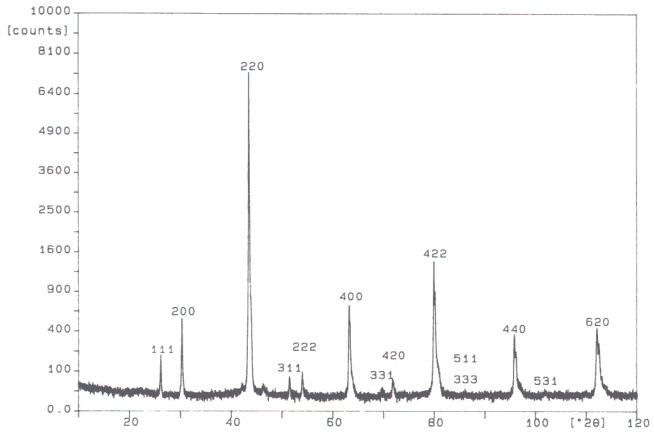

Fig. 4—X-ray diffraction pattern of β'-phase Ni_2AlTi powders.

a consequence of segregation due to nonequilibrium solidification during the atomization process, causing the ternary eutectic reaction $L \leftrightarrows \gamma' + \beta' + \eta$.

The powders intended to be pure β and β' gave X-ray patterns consistent with the expected structure; both powders exhibited strong superlattice lines, like the (100) reflection of β (B2) phase in Figure 3 and the (111) reflection of the β' $L2_1$ phase in Figure 4. It is likely that the β and β' phases are ordered, probably from the temperature of their formation.

B. *Optical Microstructures*

The intensity with which Kalling's solution attacked each phase decreased in the order β', β, and γ', with the identification of each phase being confirmed using microanalysis. Figures 5(a) through (d) show both the longitudinal and transverse optical microstructures of

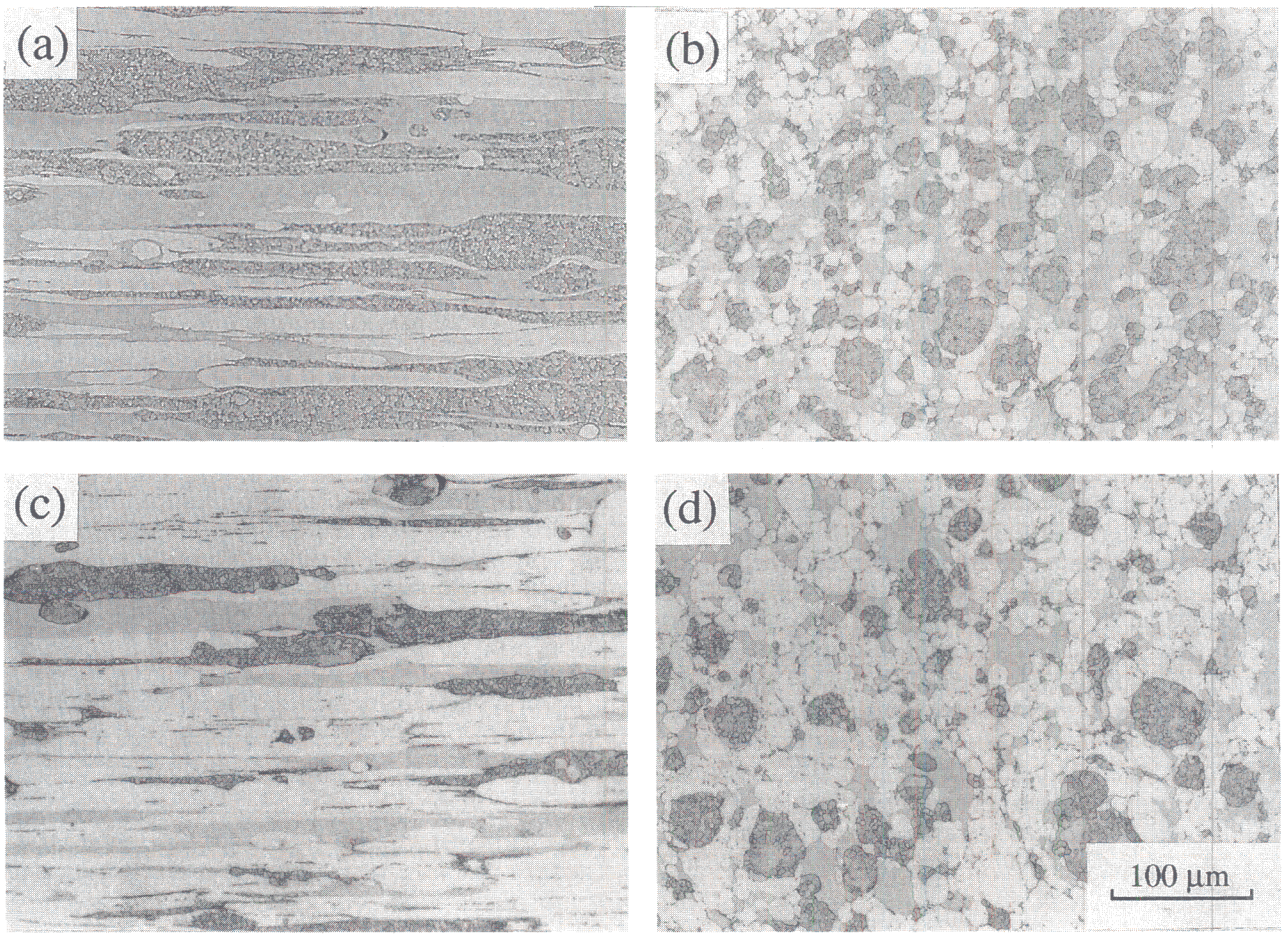

Fig. 5—Longitudinal and transverse optical microstructures of as-extruded (*a*) and (*b*) MeMeC *B* and (*c*) and (*d*) MeMeC *C*: γ' phase (white), β phase (gray), and β' phase (black).

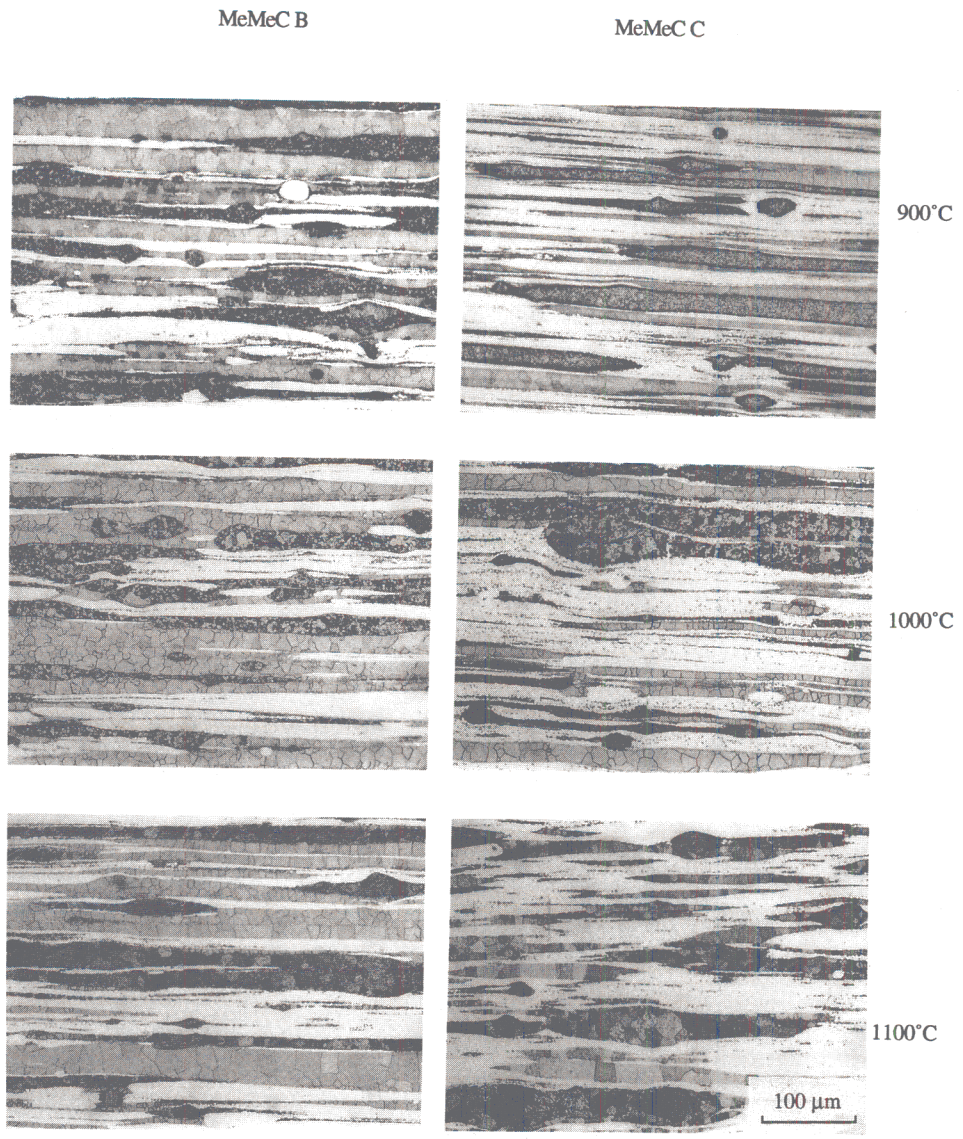

Fig. 6—Longitudinal microstructures of MeMeC *B* and *C* after 1 h heat treatment at 900 °C, 1000 °C, and 1100 °C.

as-extruded MeMeC *B* and MeMeC *C* samples, respectively. As expected, the microstructure has a fibrous morphology along the extrusion direction, and the proportion of the matrix phase, γ', (75 wt pct) in MeMeC *C* is clearly larger than that of MeMeC *B* (50 wt pct). Consistent with the aims of the experiment, the β and β' phases are intimately mixed with the γ' phase. The aspect ratios of the β and β' fibers in MeMeC *B* are higher than those of MeMeC *C*; this might be attributed to the different extrusion ram speeds by which they were fabricated (Table III). Although there is a wide range of grain size in both β and β' phases, generally the grain size of the β phase is larger than that of β'. The grain boundaries were not clear in the γ' phase, which always etched lightly. The γ' matrix was found to contain some precipitates, the intensity of precipitation apparently being larger in MeMeC *C*.

From the metallographic observations, the β phase is more deformable during extrusion compared to the β' phase. The transverse sections show that the β' phase remains nearly round in shape, whereas the β phase always filled in the gaps between the β' and γ' phases. All these observations are consistent with the fact that the highly ordered β' phase is harder than the β phase.

Some porosity could be found in all samples, located primarily along the γ'/β' and γ'/β phase interfaces. X-ray analysis of the as-extruded MeMeC's showed these to be composed of β, β', and γ' phases, together with η phase, with no significant changes caused by the fabrication process.

Experiments were conducted to examine the stability of the artificially generated microstructure. The microstructures did not change much after an hour of heat treatment at 900 °C, 1000 °C, and 1100 °C (Figure 6). The three-phase structure persisted, but precipitation occurred in the β/β' phase after heat treatment at 1100 °C. The fiber character of the β and β' phases did not change at this temperature. The microstructural changes were most severe after heat treatment at 1100 °C, but the fibrous structure was retained in all cases; however, there was some coarsening of the β and β' phase grain size

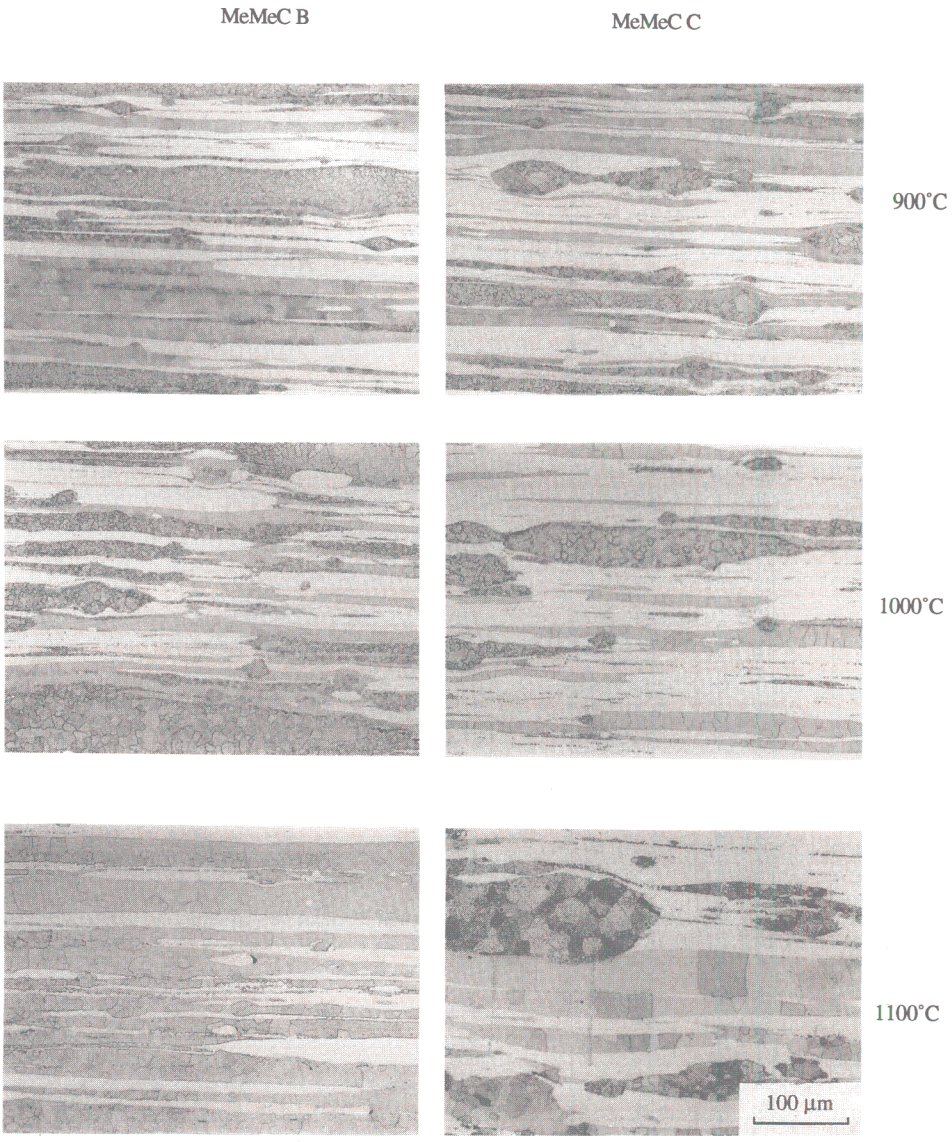

Fig. 7—Longitudinal microstructures of MeMeC *B* and *C* after 3 h heat treatment at 900 °C, 1000 °C, and 1100 °C.

with increasing heat treatment temperature. Some grains in the β phase were found to grow across the β phase fibers, giving the appearance of a bamboo structure (Figure 6).

Figure 7 shows the microstructures after heat treatment at 900 °C, 1000 °C, and 1100 °C for 3 hours. The prolonged heat treatment makes the β and β' phases less distinguishable for all temperatures, but during heat treatment at 1100 °C, the phases become less distinguishable because of their interprecipitation. The fiber character of the microstructure persisted throughout. The results from some particularly long-term heat treatments are shown in Figures 8(a) through (c). MeMeC *B* and *C*, heat-treated for 2730 hours at 1000 °C, had microstructures in which the three phases are clearly distinguishable. Some particles precipitated along the grain boundaries or within the β phase (Figures 8(a) and (b)).

Figure 8(c) shows the microstructure of MeMeC *C* after heat treatment at 900 °C for 2500 hours. The fiber structures of the β and β' are almost destroyed, but the three phases are still distinguishable.

C. *Phase Chemistries*

The fine-scale precipitation reactions that can be found even in the as-extruded samples should affect the accurate determination of the compositions of the matrix using scanning electron microscopy. Nevertheless, the energy dispersive X-ray analysis can still reveal any tendency for composition change. In principle, higher resolution experiments can be done using transmission electron microscopy, but, in spite of intense effort, we have found it impossible to make thin foils using either electropolishing or ion–beam thinning.

Figures 9(a) and (b) illustrate the observed composition changes in MeMeC *B* and *C*, bearing in mind that the analysis technique has a microanalytical resolution consistent with an SEM. As the heat treatment temperature is increased, there is an obvious tendency for the nickel concentration to increase and the aluminum concentration to decrease in both the β and β' phases. However, the γ' composition did not change much, so it seems reasonable to conclude that it is the precipitation of γ'

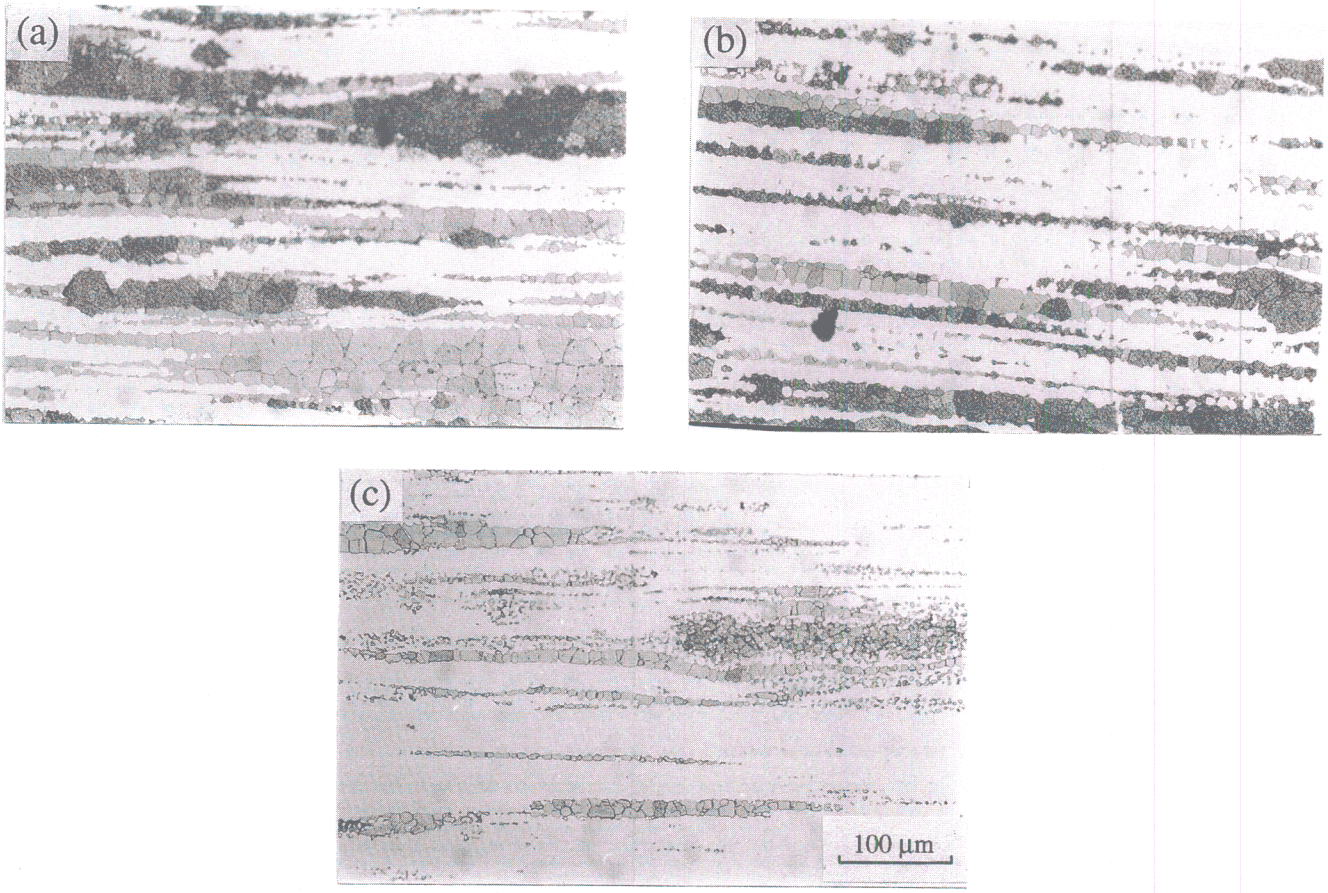

Fig. 8—Longitudinal microstructures of MeMeC *B* and *C* after long-term heat treatment. (*a*) MeMeC *B*, 1000 °C, 2730 h; (*b*) MeMeC *C*, 1000 °C, 2730 h; and (*c*) MeMeC *C*, 900 °C, 2500 h.

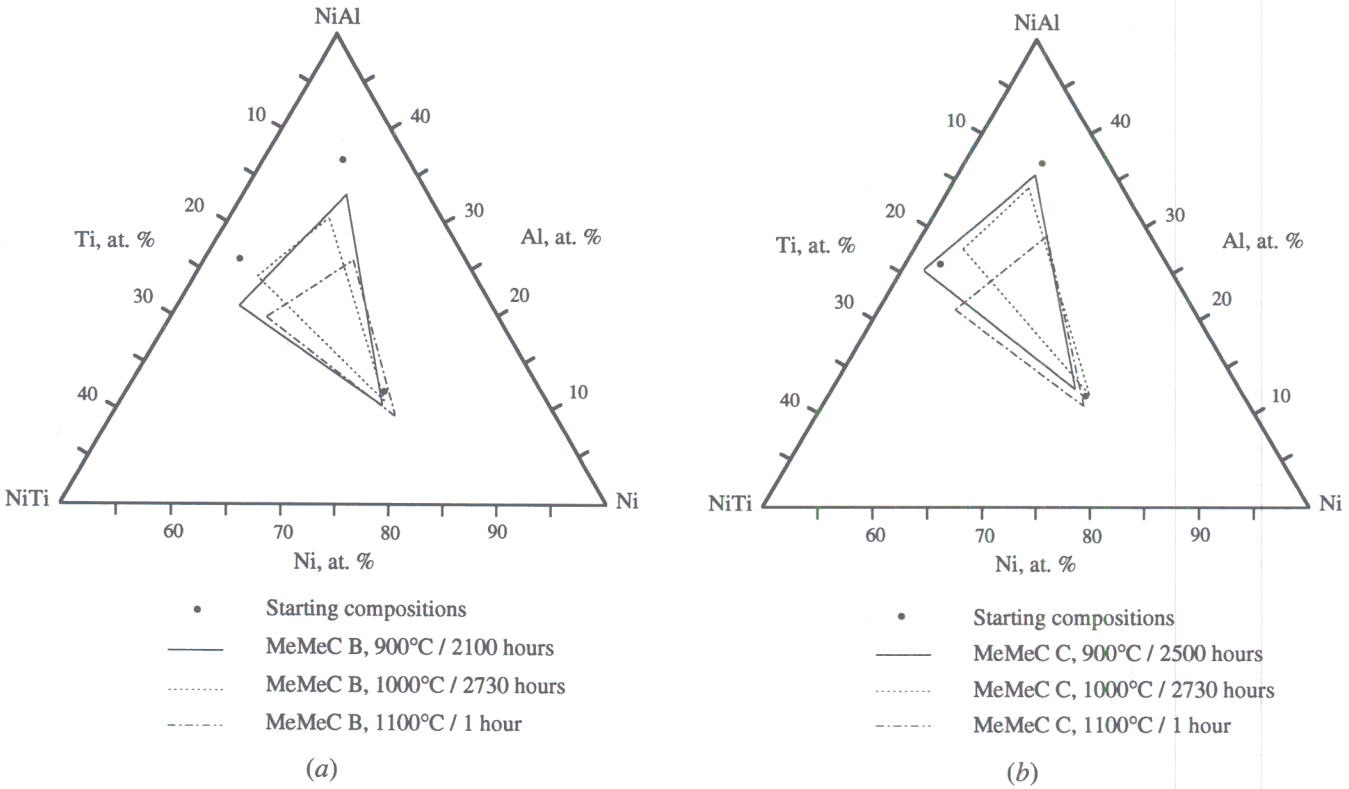

Fig. 9—(*a*) Composition changes in the β, β', and γ' of MeMeC *B* after heat treatment; (*b*) composition changes in the β, β', and γ' of MeMeC *C* after heat treatment.

Table IV. Compression Test Data for MeMeC *C* (Ni-18.24Al-14.11Ti, Atomic Percent) Heat-Treated 3 Hours at 1100 °C with Those of Alloys H5 and H6[5]

Alloy	Direction	Temperature (°C)	0.2 Pct CYS* (MPa)	UCS** (MPa)	Strain (Pct)
MeMeC *C*	longitudinal	room temperature	1200	2422†	13.9
	transverse	room temperature	1030	2785†	23
	longitudinal	700	910	1341	>34.6‡
	longitudinal	700	757	1274	>22.5‡
H5 alloy§	—	room temperature	1025	—	12.9
	—	800	688	—	15.0
H6 alloy¶	—	room temperature	1023	—	6.1
	—	700	1184	—	17.1

*Compression yield strength.
**Ultimate compression strength.
†Fracture.
‡Test interrupted.
§Ni-20Al-13Ti (at. pct) + 0.1 wt pct *B*.
¶Ni-19Al-12.35Ti-5Fe (at. pct) + 0.1 wt pct *B*.

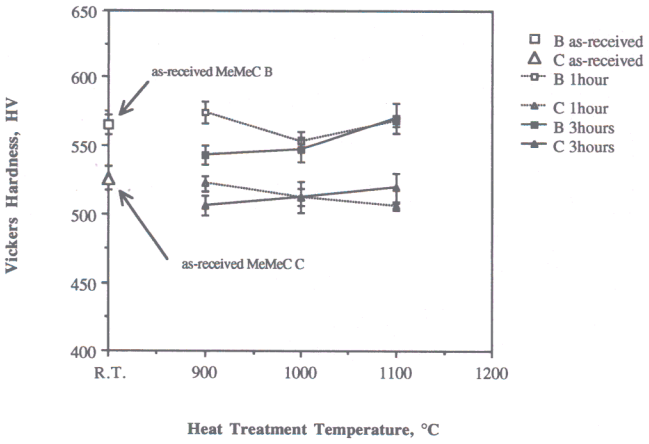

Fig. 10 — A plot of the hardness of MeMeC *B* and *C vs* heat-treatment temperature plot. Each heat treatment was for a period of 1 and 3 h.

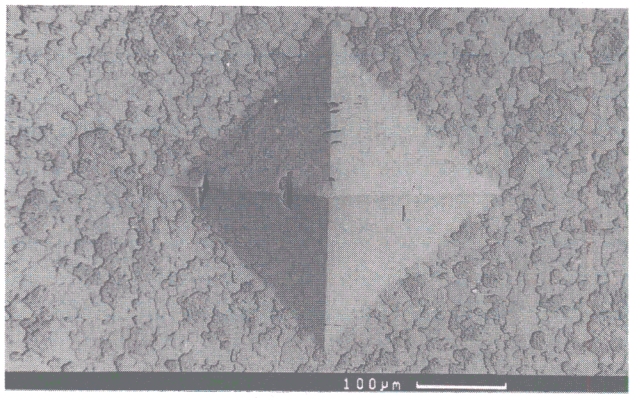

Fig. 11 — Hardness indentation loaded with 20 kg in the as-extruded MeMeC *B*.

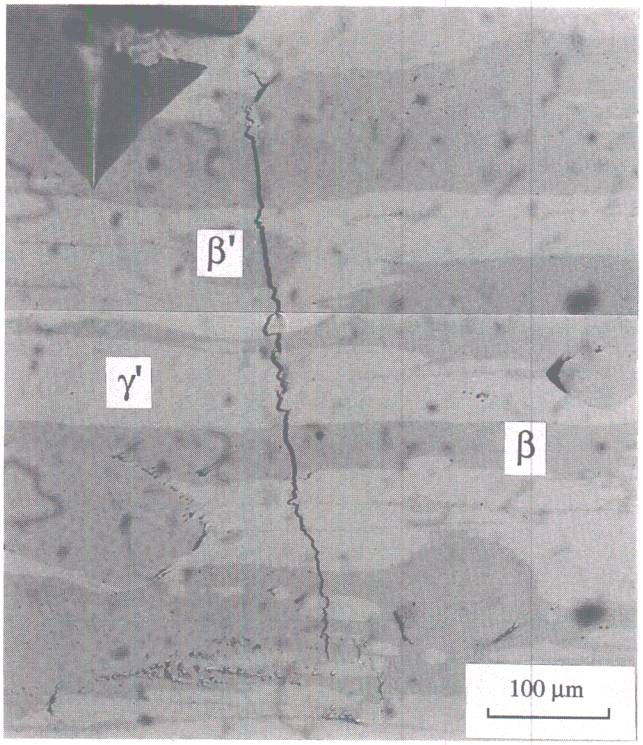

Fig. 12 — Indentation crack propagating through β, β', and γ' phases in the as-extruded MeMeC *C* alloy.

in the β or β' phase that is responsible for the observed changes. Indeed, it is expected that there should be an increase in the fraction of γ' as the heat-treatment temperature increases. The compositions of the β and β' phases thus *appear* to become nickel-rich. Also, from Ni-Al binary phase diagram, the composition range of the β (NiAl) phase is relatively wide (45 to 70 at. pct Ni at 1395 °C) compared with that of γ' (Ni_3Al). It might be deduced that the single NiAl phase in the ternary phase diagram has high nickel solubility as well, so the β corner of the tie-triangle would move toward the nickel-rich direction.

D. *Mechanical Properties*

The hardness results, after heat treatment for 1 and 3 hours at 900 °C, 1000 °C, and 1100 °C, are shown in Figure 10. The first thing to note is that in absolute terms,

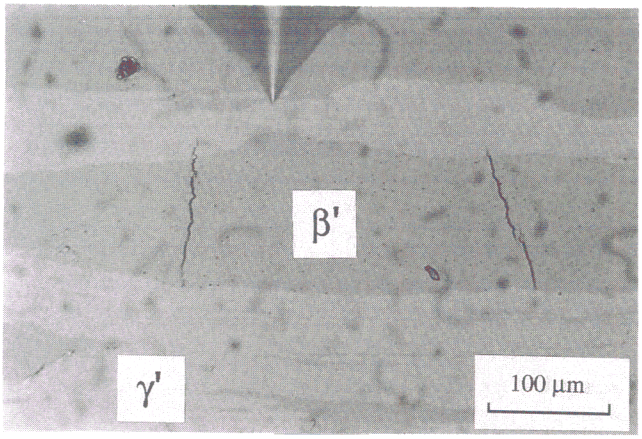

Fig. 13—Crack tip stopped at the γ' phase.

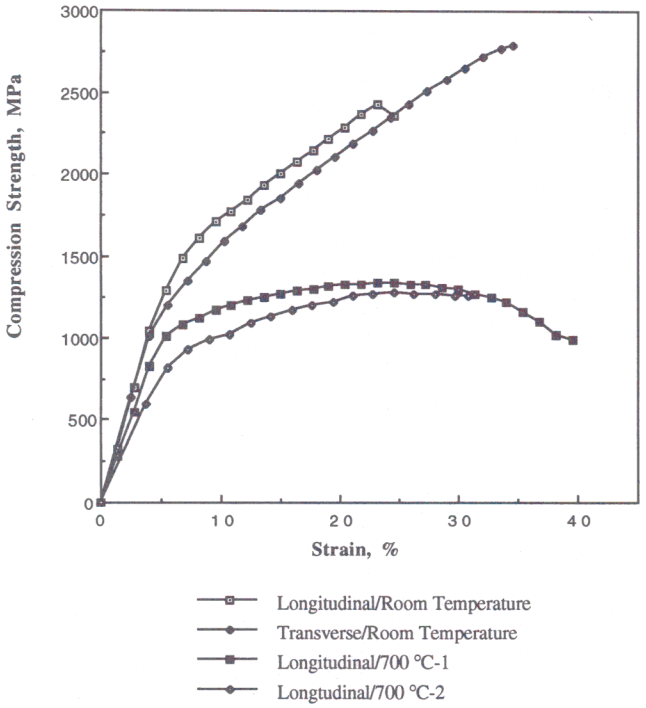

Fig. 14—Compression stress-strain curves of MeMeC *C* (75γ'-15β-15β', wt pct) after heat treatment at 1100 °C for 3 h.

the changes observed are not very large at all. The small changes are difficult to interpret since the microstructural information is not available on a fine enough scale. However, some speculative interpretation is presented subsequently; the main point is that there is no major loss in strength in spite of some quite severe heat treatments.

When heat treated for 3 hours, the hardness of both MeMeC *B* and *C* increased with the heat-treatment temperature. It is believed that the increase in the hardness of MeMeC *B* during prolonged heat treatment is due to the fine precipitation of γ'; such precipitation is more pronounced in MeMeC *B* because it contains a smaller starting volume fraction of γ'.

Figure 11 shows a typical Vickers hardness indentation during testing. Cracks could not be found in most

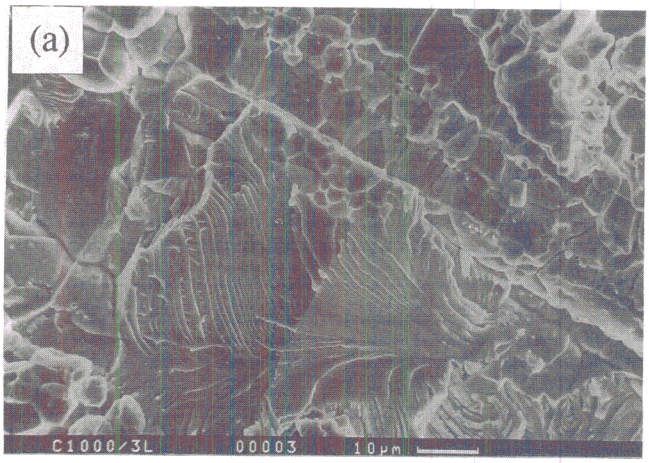

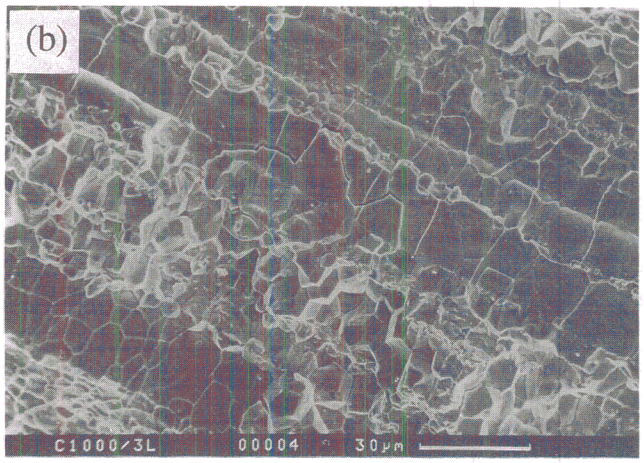

Fig. 15—Fracture surfaces of the MeMeC *C* after compression testing at room temperature along the longitudinal direction, exhibiting (*a*) transgranular and (*b*) intergranular fracture modes.

tests. By deliberately overloading (from 20 to 50 kg), it was possible to observe indentation fracture, with three interesting features. As shown in Figure 12, crack propagation in the β or β' phases was usually transgranular and the propagation path nearly planar. By contrast, the cracks tended to be more convoluted when passing through the γ' phase, with a distinctly intergranular fracture mode. Crack tips often stopped at the γ' phase (Figure 13). These results support the intended role of the γ' phase, that of enhancing ductility by arresting cracks.

Figure 14 shows the compression stress-strain curves of the MeMeC *C* after heat treatment at 1100 °C for 3 hours, and the detailed results are listed in Table IV. It is surprising that the plastic strain is up to 13.9 pct in the longitudinal direction at room temperature and 23 pct in the transverse direction. MeMeC *C* is more ductile at higher temperature. Tests conducted at 700 °C were stopped as the strain exceeded 22.5 pct, since microcracking then began to contribute to the measured ductility. The compression yield strength was somewhat smaller in the transverse direction but with higher values of the ultimate compression strength (UCS), 2785 MPa, and the room temperature ductility, 23 pct.

Table IV also contains published data[5] from similar alloys tested with the same conditions but made *via* the

conventional casting and precipitation route. One unique feature of alloys H5 and H6 is that they were doped with boron or iron (0.1 wt pct boron in H5 and 5 at. pct iron + 0.1 wt pct boron in H6) for greater ductility, and in fact, the ductility of alloy H5 (12.9 pct) tested at room temperature is the largest of all reported values. Yang *et al.*'s results on H6 show that the strength increases with temperature. They explained this in terms of the well-established increase in γ' strength with temperature. However, our results for MeMeC *C*, which contains a larger amount of γ', do not show an increase in the yield strength with temperature. This result is not understood.

Figures 15(a) and (b) show both transgranular and intergranular fracture components. More than 90 pct of the fracture surface shows intergranular fracture (Figure 15(a)). The weak bonding at the interphase interfaces is the likely cause of such failure, with debonding along a row of grains which belong to a single phase, as illustrated in Figure 15(b).

IV. CONCLUSIONS

An initial study has demonstrated that highly stable microstructures can be engineered by coextruding powders consisting of single phases whose compositions are chosen so as to encourage equilibrium in the final microstructure. For the specific system studied here, considerable ductility has been observed in compression tests, both at ambient and elevated temperatures. The ductility is found to be larger than ever reported before and at fairly high strength levels, even at temperatures as high as 700 °C.

There are obvious ways in which this work needs to be supplemented. For example, no attempt has been made to optimize the extrusion conditions, to refine the particle size before extrusion, to dope either individual phases or the extrudate as a whole with grain boundary strengthening elements, to add oxide dispersions, *etc.*

ACKNOWLEDGMENTS

We wish to thank Professor C. Humphreys for the provision of laboratory facilities in this department. Thanks are also extended to Dr. K. Mino for providing alloy powders, and to INCO, United Kingdom, for extruding them. One of us (LCH) would like to thank the Chung-Cheng Institute of Technology in Taiwan, Republic of China, for its financial support. HKDHB's contribution was made under the auspices of the "Atomic Arrangements: Design and Control" Project, which is a joint venture between the Japan Research and Development Corporation and the University of Cambridge.

REFERENCES

1. G. Thomas: *Metall. Trans. A*, 1978, vol. 9A, pp. 439-50.
2. H.K.D.H. Bhadeshia and D.V. Edmonds: *Met. Sci.*, 1979, pp. 325-34.
3. L.S. Sigl and H.E. Exner: *Metall. Trans. A*, 1987, vol. 18A, pp. 1299-1308.
4. L.S. Sigl, P.A. Mataga, B.J. Dalgleish, R.W. McMeeking, and A.G. Evans: *Acta. Metall. Mater.*, 1988, vol. 36, pp. 945-53.
5. R. Yang, J.A. Leake, and R.W. Cahn: *Mater. Sci. Eng.*, 1992, vol. A152, pp. 227-36.
6. R. Yang, N. Saunders, J.A. Leake, and R.W. Cahn: *Acta. Metall. Mater.*, 1992, vol. 40 (7), pp. 1553-62.
7. P.S. Khadkikar, K. Vedula, and B.S. Shabel: *Mater. Res. Soc. Symp. Proc.*, 1987, vol. 81, pp. 157-64.